Self-Calibrated MEMS Gyroscope with AM/FM Operational Modes, Dynamic Range of 180 dB, and In-Run Bias Stability of 0.1 deg/hr

S.A. Zotov, I.P. Prikhodko, B.R. Simon, A.A. Trusov, A.M. Shkel

MicroSystems Laboratory, University of California,

Irvine, CA,
USA

Inertial Sensors and Systems 2014

Karlsruhe, Germany

Abstract

This paper reports our cumulative progress toward the development of a gyroscope with two interchangeable modes of operation: an Amplitude Modulated (AM) mode, for a precision measurement in more conventional ranges (~300 deg/sec) and a Frequency Modulated (FM) mode, for an expanded range of operation (over 300 deg/sec and as high as 18,000 deg/sec). We demonstrate that the implemented self-calibration algorithms for AM detection effectively remove the rate random walk, allowing for a highly stable in-run bias. The FM approach is based on tracking the resonant frequency split between two, high Q-factor mechanical modes of a gyroscope, providing a frequency-based measurement of the input angular rate. Temperature characterization of the FM gyroscope exhibited less than 0.2 % variation of the angular rate response between a temperature range of 25 °C and 70 °C. This characteristics is shown to be enabled by the self-calibration capability of differential frequency detection. Measured Allan deviation of the FM gyroscope demonstrated a bias instability of 0.5 °/hr and an Angle Random Walk (ARW) of 0.08 °/√hr. Rate table characterization of the gyroscope in FM operational mode demonstrated a linear range of 18,000 °/s, representing a dynamic range of 160 dB. In the conventional AM mode, the gyroscope experimentally demonstrated a 0.1 °/hr bias instability after implementation of the temperature self-sensing calibration algorithm. Thus, the interchangeable operation of the QMG transducer provides a measured 176 dB dynamic range, making the same high-Q mechanical structure suitable for demanding high precision and wide input range applications.

1. Introduction

A majority of commercial MEMS vibratory gyroscopes are angular rate measuring sensors, which employ energy transfer between two modes of vibration in response to inertial rotation [1], [2]. While angular rate information with moderate accuracy and stability is sufficient for motion detection and stabilization in consumer electronics and some automotive application, precision angular position and continuous orientation tracking with high precision and stability is required for typical inertial navigation, the North tracking, dead-reckoning, and targeting systems [3]. Moreover, wide input range and high measurement bandwidth are also critical for pointing and missile guidance systems, especially in harsh and GPS-denied environments. Although conventional fiber optic, ring laser, and hemispherical resonator gyroscopes can in principle satisfy some of the requirements, their miniaturization is challenging. The emergence of silicon microelectromechanical (MEMS) gyroscopes capable of precision and wide dynamic range

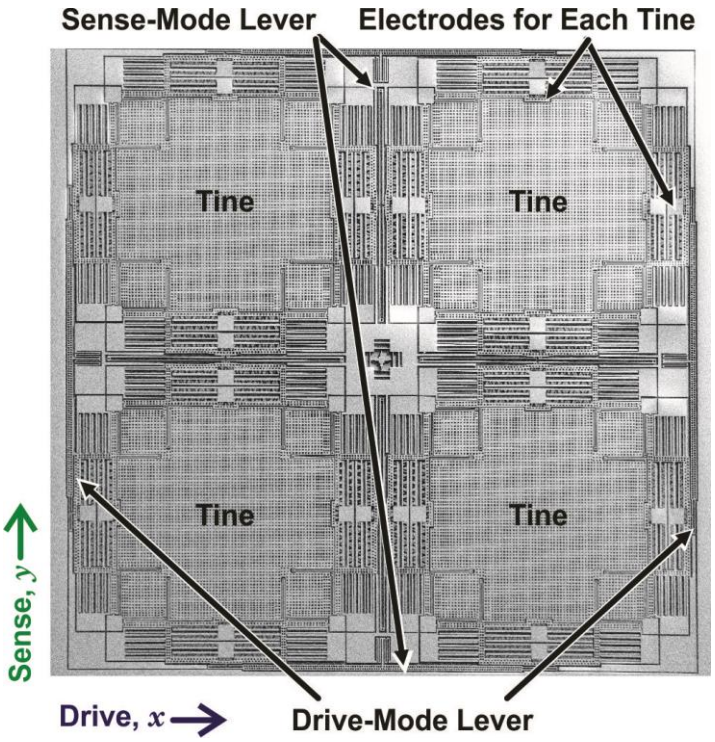

Figure 1. SEM image of a fabricated 100 μm SOI quadruple mass gyroscope (QMG). Die size is 8.6 × 8.6 mm.

measurements of both angular velocity and position (angle) is highly desirable. A few authors have already reported feasibility of precision rate gyroscopes with a sub-degree per hour in-run bias instability [4]–[10].

The challenge for implementation of MEMS-based precision inertial instruments is the requirement for high quality (Q) factor, as well as structural isotropy of stiffness and damping. Recently, we proposed the interchangeable rate and rate integrating (whole-angle) operation [11], [12], making one high-Q transducer suitable for high precision and wide range measurements. Using the same transducer we also demonstrated a sub-degree per hour rate resolution [7], high input range and measurement bandwidth [13], [14], as well as a differential frequency detection robust to the temperature variations [15]. In this paper, we review each of the operational modes and discuss an interchangeable operation in a precision and high dynamic range made of the silicon MEMS sensor with a digital output, suitable for demanding inertial navigation and guidance applications. This paper summarizes our recent publications [3, 7, 11-17, 19] and intends to provide a summary of the high performance inertial MEMS development at the MicroSystems Laboratory of the University of California, Irvine during the period from, approximately, 2008 to 2012.

In the following sections we describe the gyroscope dynamics, design requirements, and experimental characterization for the each mode of operation, conventional amplitude

modulation (AM) and frequency modulation (FM). Using the same high-Q transducer structure, Figure 1, we demonstrated the operation of each mode by switching the signal conditioning and control electronics.

2. Transducer Design and Fabrication

In this section we report the transducer design, fabrication, and structural characterization.

2.1. Design Criteria

Several design criteria must be met by the mechanical sensor element to fully realize the proposed methods of operation. A geometrically symmetric and mode-matched structure is needed to optimize the minimal detectable angular rate signal and increase the temperature stability of the sensor. High Q-factor allows to achieve the resolution at the high rate and frequency stability. Identical high Q is needed in both modes of mechanical vibration to maximize the rate resolution and enable a low angle drift. These requirements are satisfied by an X-Y symmetric, dynamically balanced, anti- phase operated gyroscope, such as the Quadruple Mass Gyroscope (QMG) architecture [12], [16].

2.2. Quadruple Mass Gyroscope Architecture

The mechanical structure of the QMG mechanical sensor element comprises of four identical, symmetrically decoupled tines with linear coupling flexures, as well as a pair of anti-phase synchronization lever mechanisms for the X- and the Y-mode, Figure 1. This X-Y symmetric system of four anti-phase tines provides the structure with two anti-phase, dynamically balanced modes of mechanical vibration at a single operational frequency. The complete X-Y structural symmetry of the device improves robustness against the fabrication imperfections and temperature induced frequency drifts. An additional advantage of the QMG anti-phase levered architecture is the mechanical suppression of the parasitic common mode of in-phase displacement in the coupled tines. The same QMG architecture will be used for AM and FM modes of operation reported in this paper.

2.3. Fabrication and Packaging

The QMG prototypes, Figure 2, were fabricated using an in-house, wafer-level, single-mask process based on Silicon-on-Insulator (SOI) substrates with 100 μm thick device layer and a 5 μm buried oxide layer. Sensors were defined in a highly doped (boron concentrations of 10^{20} cm^{-3}) device layer by Deep Reactive Ion Etching (DRIE). Stand-alone sensors were vacuum sealed using a package-level technology for robust vacuum

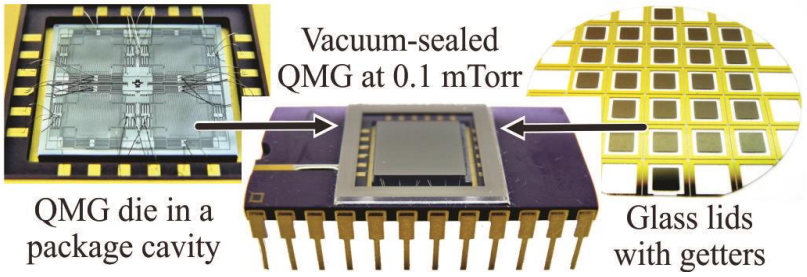

Figure 2: Photograph of a vacuum packaged QMG used in the experiments. Insets: die before sealing; glass lid wafer.

sealing [17]. First, the gyroscope die was attached to a ceramic package using eutectic solder, and then wire bonded. The device was sealed at sub-mTorr vacuum, preceded by a getter activation on a glass lid.

2.4. Structural characterization

The dynamically balanced anti-phase design and vacuum packaging of QMG sensors were expected to yield isotropic high Q factors for stable AM and FM operation. The structural X- and Y-modes of a vacuum-sealed QMG prototype were experimentally characterized at different temperatures using ring-down tests in a TestEquity 107 thermal chamber. Exponential fits of the time-domain amplitude decay data showed time constants of τ_x = 167.1 s and τ_y = 168.8 s for the X- and Y-modes, respectively, confirming structural and damping symmetry, with $\Delta(1/\tau) = 6\times10^{-5}$ s^{-1}, Figure 3. This value of time constant allows to observe free gyroscope dynamics during several minutes. The Q factors were calculated by the formula $Q = \pi f_n \tau$, with the measured natural frequency f_n = 2.2 kHz.

A Q-factor of X- and Y-modes of 1.16 million approached the fundamental thermo-elastic limit of 1.3 million, derived from the Finite Element Modeling (FEM) of the structure. Characterization of Q factors over the temperature range from -40 ºC to +100 ºC is shown in Figure 4. For T > 0 ºC, the data exhibit $1/T^3$ dependence, which is characteristic of thermoelastic dissipation [18]. Below 0 ºC, the device's Q factor levels off at approximately 1.7 million, attributed to anchor loss caused by slight structural imbalances. A more detailed analysis of anchor loss due to structural imbalances in tuning-fork MEMS is reported in [19].

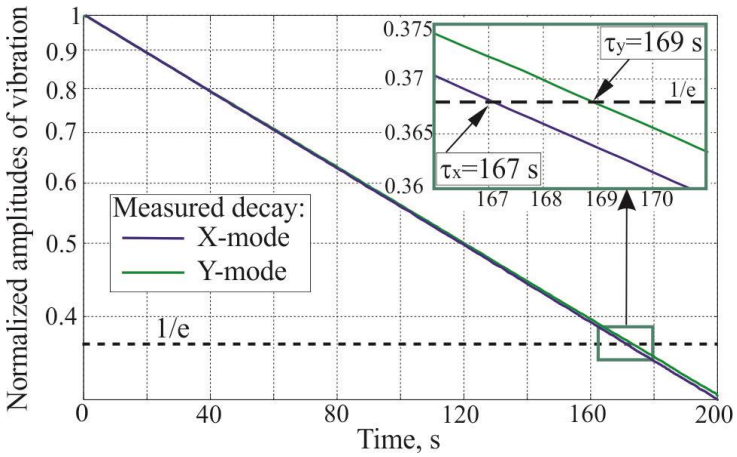

Figure 3. Experimental characterization of the packaged QMG using ring-down test, revealing identical Q factors for both modes (with ΔQ/Q of 1%).

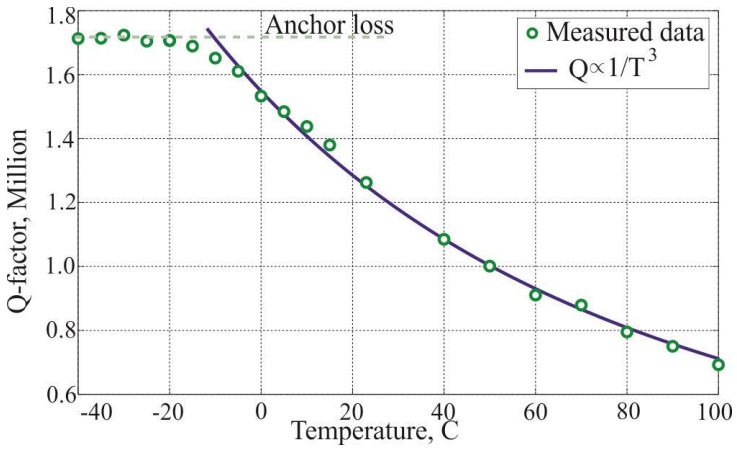

Figure 4. Measured Q factor versus temperature for QMG, showing $1/T^3$ dependence of thermoelastic dissipation for T > 0 ºC.

3. Frequency Modulated Mode

In this section, we analyze the often ignored effect of mechanical FM in vibratory gyroscopes, formulate a new FM based principle of rate measurement, and analyze its properties. This section describes dynamics and experimental characterization of the QMG sensor operated in a wide range angular rate measuring mode. The operating principle is based on mechanical frequency modulation of an input rate previously introduced in [15].

3.1. Frequency Based Detection of Input Rate

The QMG rate sensor in Frequency Modulation (FM) operation mode could eliminate the gain-bandwidth and dynamic range trade-off of conventional AM gyroscopes and enable signal-to-noise ratio improvements by taking advantage of high-Q mechanical element without limiting the measurement bandwidth. In contrast to conventional rate measuring mode, the dynamics of FM-operated gyroscope is based on free vibrations of the inertial

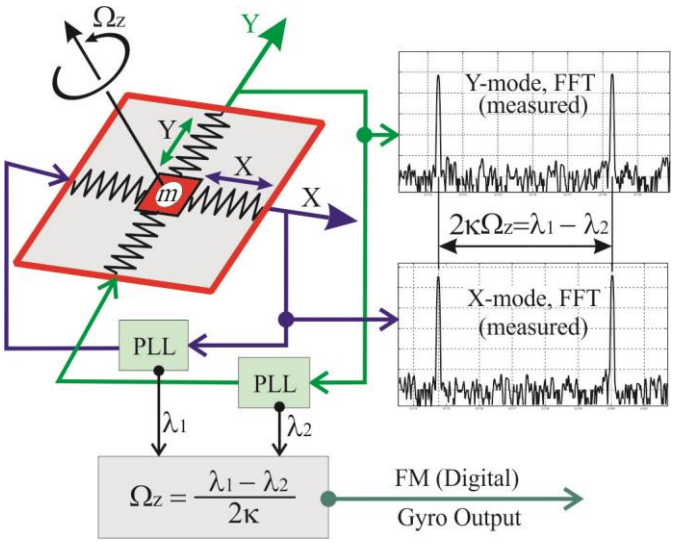

Figure 5. Schematic and operating principle of a gyroscope for wide range angular rate measurements (frequency modulation mode of operation). The operation is based on the mechanical frequency modulation of the inertial input. The input rotation causes a frequency split between the gyroscope's X-mode and Y-mode, producing a FM measure of the input rate.

mass, when both X- and Y-modes are unconstrained and allowed to move freely in response to the inertial stimulus. The free vibrations dynamics of a 2-D isotropic mass-spring-damper system with the natural frequency ω and the quality factor Q in the non-inertial coordinate frame (device frame) Oxy is (Figure 5):

$$\begin{aligned} \ddot{x} + \frac{Q}{\omega}\dot{x} + \left(\omega^2 - \Omega_Z\right)x - \dot{\Omega}_Z y &= 2\dot{y}\Omega_z \\ \ddot{y} + \frac{Q}{\omega}\dot{y} + \left(\omega^2 - \Omega_Z\right)y + \dot{\Omega}_Z x &= -2\dot{x}\Omega_z \end{aligned} \tag{1}$$

Assuming negligible damping ($Q > 10^6$), the closed-form solution of equation (1) is:

$$\begin{aligned} x &= C_1 \sin\left(\omega t + \int_0^t \Omega_Z dt\right) + C_2 \sin\left(\omega t - \int_0^t \Omega_Z dt\right) + C_3 \cos\left(\omega t + \int_0^t \Omega_Z dt\right) + C_4 \cos\left(\omega t - \int_0^t \Omega_Z dt\right) \\ y &= C_1 \sin\left(\omega t + \int_0^t \Omega_Z dt\right) - C_2 \sin\left(\omega t - \int_0^t \Omega_Z dt\right) - C_3 \cos\left(\omega t + \int_0^t \Omega_Z dt\right) + C_4 \cos\left(\omega t - \int_0^t \Omega_Z dt\right) \end{aligned} \tag{2}$$

where C_i represents constants depending on initial conditions.

The solution (2) defines the gyroscope vibration as a superposition of two sinusoids with phases $\omega t + \int_0^t \Omega_Z dt$ and $\omega t - \int_0^t \Omega_Z dt$, respectively. The effective modal frequencies λ_1 and λ_2 are defined by the time derivative of the phases with respect to time:

$$\begin{aligned} \lambda_1 &= \omega + \Omega_Z, \\ \lambda_2 &= \omega - \Omega_Z. \end{aligned} \tag{3}$$

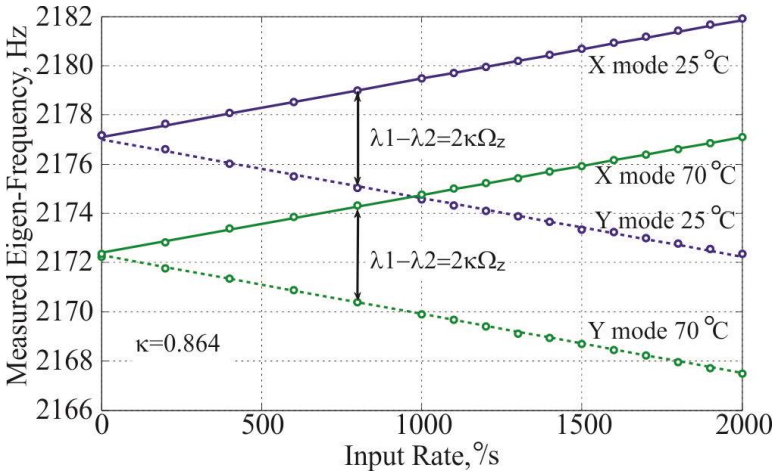

(a) Differential FM detection of the input rate from the modal frequency split ($\lambda_1 - \lambda_2$) is invariant to temperature.

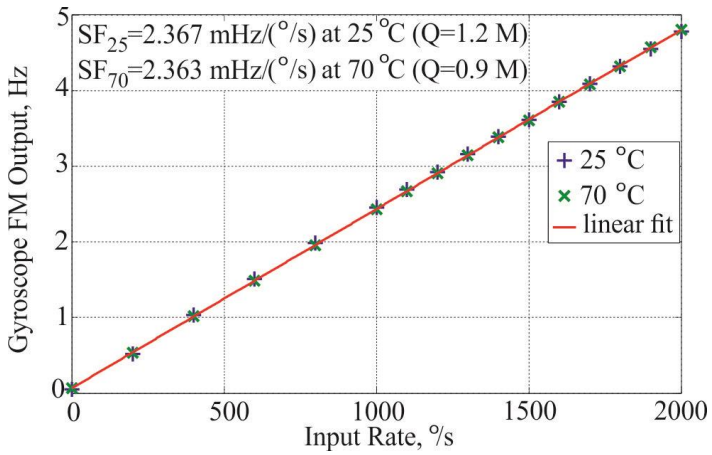

(b) Measured FM rate responses for 25 °C and 70 °C using differential detection of the modal frequency split with inherent self-calibration.

Figure 6. Rate characterization of the FM-based sensor shows no drift in the response for 25 °C and 70 °C, despite a 30 % reduction in Q-factor and a 5 Hz drop of nominal frequency.

The expression (3) defines the instantaneous modal frequencies λ_1 and λ_2 with respect to rotating reference frame OXY in the presence of arbitrary time-variant input $\Omega z \neq 0$.

The gyroscope's free vibrations contain only one frequency ω with respect to the inertial frame. At the same time, two splitting frequencies λ1 and λ2 are observed, (3), with respect to the device moving frame. The FM effect is inherent to the moving reference frame and enables measuring the input rate Ωz from the observed split in the instantaneous modal frequencies.

Based on the eigenfrequency solution, (3), for an initially mode-matched gyroscope, the input rotation rate Ωz can be measured from the observed modal frequencies λ1 and λ2 according to a linear expression:

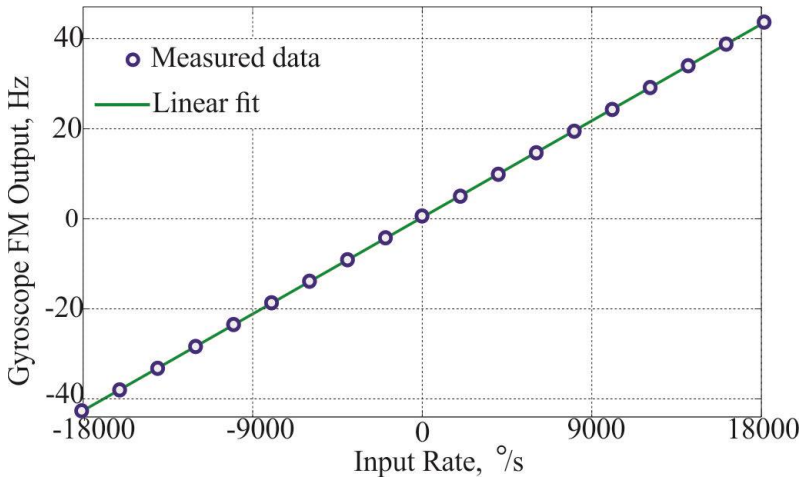

Figure 7. Characterization of the FM-based rate sensor reveals less than 0.2 % of nonlinearity in wide input range of 18,000 °/s.

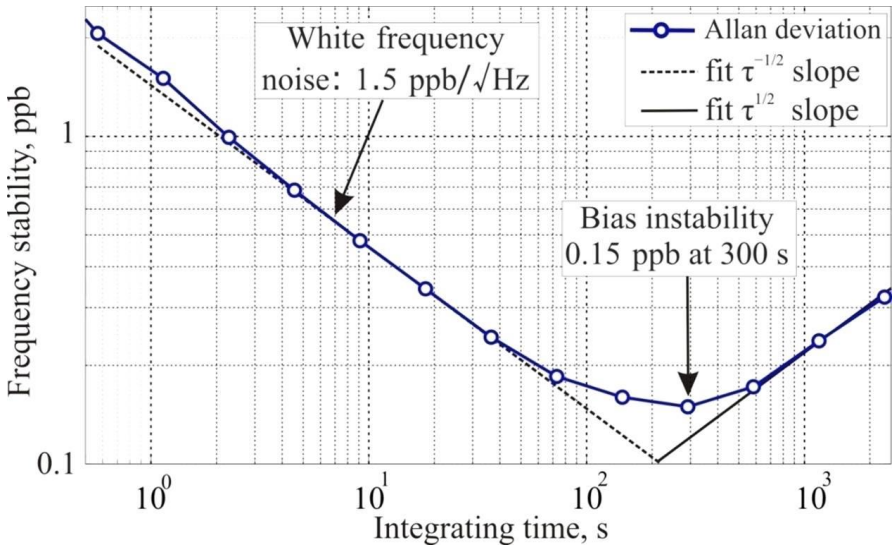

Figure 8. Measured Allan variance of the FM sensor showing 1.5 ppb/√Hz ARW and 0.15 ppb bias instability, which translates to 5 °/hr/√Hz ARW and 0.5 °/hr gyroscope bias instability.

$$\Omega_Z = \frac{1}{2}\left(\lambda_1 - \lambda_2\right), \quad (\text{for } \Delta\omega = 0) \tag{4}$$

The proposed FM-based operational principle can also be extended to the more general case of a gyroscope with an initial frequency mismatch ($\Delta\omega > 0$), see for details [15].

The obtained closed-form solutions, (3) and (4), provide the basis for the frequency-based measurement of the input rate by tracking the modal frequency split at a high Q-factor, nearly mode-matched, vibratory gyroscope. The quasi-digital FM approach resolves the Q versus linear range and bandwidth tradeoff of conventional analog AM-based vibratory rate sensors. Maximization of the FM-operated gyroscope Q-factor improves the frequency stability and rate resolution. At the same time, the linear input range of an FM-operated gyroscope is independent of the Q and is only limited by the device nominal frequency

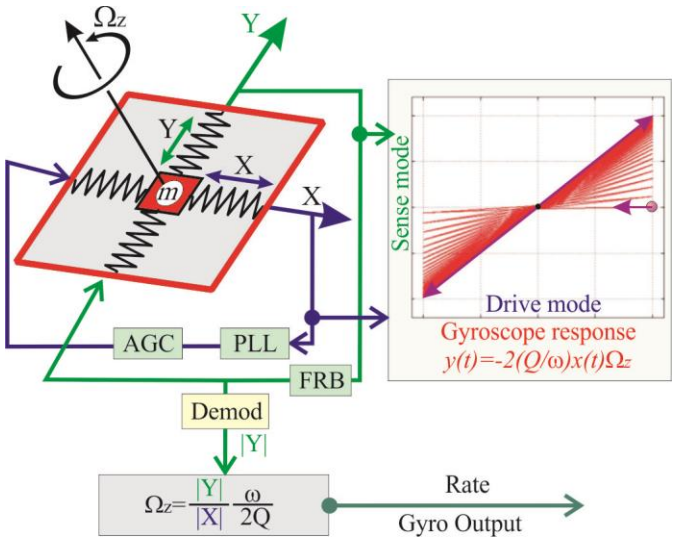

Figure 9. Schematics and operating principle of a gyroscope for angular rate measurements (conventional amplitude modulation mode of operation). The axis of vibration is locked to the intended drive direction. The inertial rotation induces the motion in the sense direction, with the amplitude proportional to an input angular rate.

($\Omega_Z < \omega$). The modal frequency split provides an instantaneous measure of the input rate, allowing the use of high-Q structures without the sensor bandwidth sacrifice. An additional advantage of the approach is the self-calibration against common drifts in the modal frequencies enabled by the differential frequency measurement (i.e., $\lambda_1 - \lambda_2$).

3.2. Experimental Characterization of FM Operation

In conventional AM mode, drift of resonant frequency and Q-factors are major sources of scale factor variations and bias drifts over temperature. Theoretical analysis of the proposed FM rate sensor suggest immunity against these drift mechanisms by virtue of the differential frequency detection, i.e. by measuring the frequency (3), (4). To experimentally investigate this hypothesis, a vacuum packaged QMG sensor operated in FM mode was characterized on a temperature controlled Ideal Aerosmith 1291BR rate table at 25 °C and at 70 °C. For these experiments, the X- and Y- modes of the QMG-device were electrostatically excited into resonance, using a combination of 0.1 Vdc bias and 0.1 Vac driving signals produced by digital PLLs. The motional signals for both modes of vibration were detected using capacitive detection with Electro-Mechanical amplitude Modulation (EAM). The two modal frequencies of the gyroscope mechanical structure were continuously monitored by the two PLLs, Figure 5. As it is theoretically expected for a mode-matched gyroscope, the measured split between the nominally equal modal frequencies was directly proportional to the input rate, Figure 6(a). Unlike the conventional

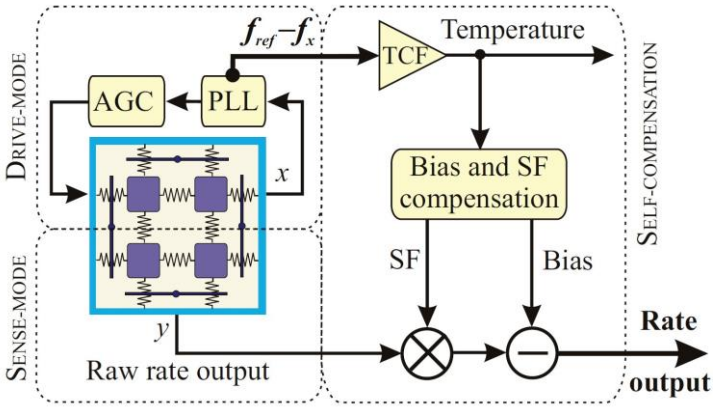

Figure 10. Signal processing using drive-mode frequency for self-compensation of temperature-induced bias and scale-factor drifts.

AM approach, the FM detection of the input rate from the modal frequency split demonstrated invariance to changes in temperature and Q-factors, Figure 6(b). Without any active temperature compensation, experimental characterization of the FM angular rate sensor at 25 °C and 70 °C revealed less than 0.2% response fluctuation despite a 30 % reduction of the Q-factor and a 5 Hz drop of the nominal frequency (caused by temperature dependency of Young's modulus). The proposed FM gyroscope operation also suggests a wide sensor input range, limited only by the device natural frequency (for $\Omega_Z < \omega$). In order to experimentally investigate this hypothesis, a vacuum packaged QMG was mounted on an Ideal Aerosmith High-Speed Position and RateTable System 1571, and characterized from 0 to 18,000 °/s (i.e., 50 revolutions per second). Without any compensation, the FM gyroscope demonstrated less than 0.2 % nonlinearity throughout the entire range, Figure 7. Noise performance of the FM sensor is limited by the frequency stability of the two modes of vibration in the gyroscope. Figure 8 demonstrates the Allan variance of the FM sensor, measurements showing a 5 °/hr/√Hz ARW and 0.5 °/hr gyroscope bias instability, resulting in a dynamic range of 160 dB in FM operation mode.

4. Conventional Angular Rate Mode

This section describes dynamics and experimental characterization of the QMG sensor operated in conventional rate measuring mode [7]. The operating principle is based on amplitude modulation of an input rate employed in most commercially available MEMS rate sensors. The dynamic analysis below assumes that gyroscopes are 2-D isotropic mass-spring-damper systems with the natural frequency ω and the quality factor, Q.

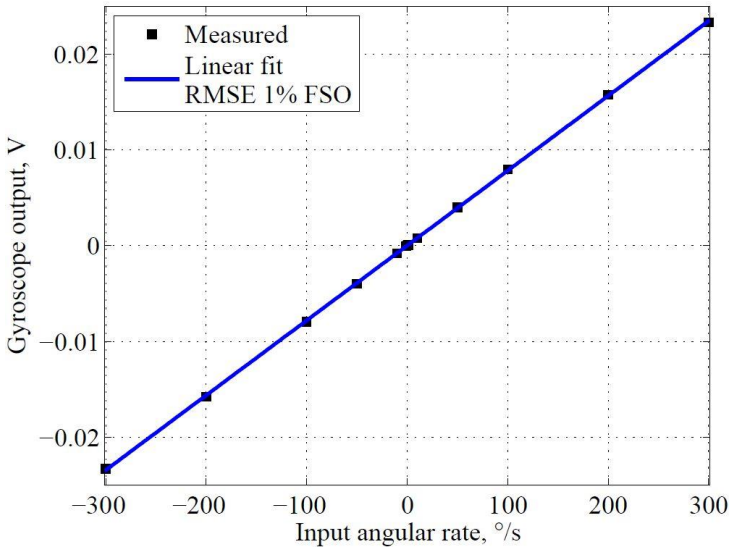

Figure 11. Measured response of the QMG sensor in the rate measuring mode, revealing a 300 º/s input range with 1% RMS nonlinearity of FSO.

4.1. AM Principle of Operation

The operating principle of a vibratory z-axis angular rate gyroscope is based on energy transfer between two vibratory modes. The drive-mode, x-axis, is continuously excited at resonance, and the sense-mode, y-axis, is used for rate detection, Figure 9. The amplitude of the sense-mode, *y*, motion is proportional to the angular rate, Ω_z, with the angular gain factor ($0 < k \leq 1$, depending on geometry) and the drive amplitude, *x* [7]:

$$y = Q_{Eff} k \Omega_Z x / \omega_y , \tag{5}$$

where ω_y is the sense-mode natural frequency. Here, Q_{eff} is the gain of the sense-mode at the drive-mode frequency ω_x:

$$Q_{Eff} = Q_y / \sqrt{1 + 4Q_y^2 (\Delta\omega / \omega)^2} , \tag{6}$$

which reaches the maximum, Q_y, at zero frequency mismatch between ω_x and ω_y, ($\Delta\omega$ = 0).

It follows from (5) that the rate sensitivity is improved by maximizing the Q-factor, drive amplitude, angular gain, while reducing the resonant frequency, and frequency mismatch.

4.2 Frequency Based Temperature Self-Sensing

While the gyroscope drive-mode is controlled by a Phase- Locked Loop (PLL) and an AGC loop, the open-loop sense-mode is susceptible to temperature variations. To compensate for temperature-induced scale-factor and bias drifts, we propose to use the drive-mode frequency as a built-in thermometer, which is free from any spatial or temporal thermal lag. Experimentally verified, the silicon resonator frequency changes linearly with the temperature, therefore by monitoring this change, on-chip gyroscope temperature can be

measured directly. The temperature coefficient of frequency is well defined by elastic properties and its value is fixed for a given material (e.g., silicon) [20], which allows for repeatable measurements of the temperature. Figure 10 shows signal processing for the real-time self-compensation of both scale-factor and bias drifts. The instantaneous frequency change is first correlated to the temperature using the measured TCF. Once the instantaneous temperature value is obtained, it is used to estimate (predict) the scale-factor and bias drifts in real-time. Finally, the raw gyroscope output is corrected by multiplying it with the scale-factor change, followed by subtraction of bias drifts. The gyroscope bias can be modeled as a constant (bias offset) plus a time-varying component (bias drift), which is primarily caused by the temperature fluctuations. For the first-order temperature *T* compensation, bias *b* is approximated by the sum of the offset value b_{T0} and a linear term with the coefficient β_T :

$$b(T) = b_{T0} + \beta_T \Delta T \tag{7}$$

This equation, due to the linear temperature dependence of frequency *f = f(T)*, can be represented in terms of the natural frequency change Δf :

$$b(f) = b_{f0} + \beta_f \Delta f \ , \tag{8}$$

The temperature sensitivity coefficient β_f and the constant b_{f0} are determined through the least-square linear fit to the calibration data. The frequency change Δf is used to estimate the temperature-induced bias drift *b(f)* and perform compensation in real-time. Similarly, self-compensation method is performed for the scale-factor.

4.3. Experimental Characterization of AM Operation

The low dissipation QMG sensor operated in rate measuring mode is expected to provide a low noise performance. The packaged QMG sensor with a 2 kHz resonant frequency and a 0.5 μm amplitude of motion in the drive mode performed under a 3.6 Hz frequency mismatch between the sense- and drive-modes. The input-output relationship demonstrates a linear rate response in 300 °/s input range with 1% RMSE of a full scale output (FSO), Figure 11.

The QMG noise performance was evaluated using the Allan deviation analysis. The zero rate output of the QMG sense-mode was recorded for 12 hours at a sampling rate of 28 Hz, Figure 12. Fit to the $\tau^{-1/2}$ slope (white noise) at the short integration time revealed a 0.06 °/√hr Angle Random Walk (ARW). The flicker noise reached for integration times between 400 s and 500 s, indicating a 0.11 °/hr bias instability. For times longer than 500 s the output was dominated by the $\tau^{1/2}$ random walk.

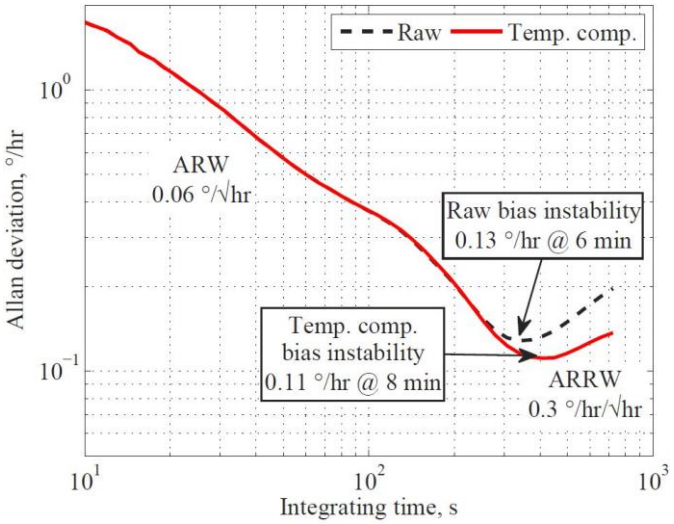

Figure 12. Measured Allan deviation of zero rate outputs, demonstrating a 0.06 °/√hr ARW and a 0.11 °/hr bias instability.

The measured 0.1 °/hr minimal resolution and the 18,000 °/s maximum input (experimentally demonstrated in the previous section by using physically the same mechanical element) of the QMG sensor provides a dynamic range of 176 dB. Further performance enhancement is possible by matching the natural frequencies of the drive- and sense-modes.

5. Discussion

The choice of a gyroscope operating mode depends upon the application requirements. For slow motion, the conventional Amplitude Modulation (AM) mode typically provides high precision and low-noise characteristics at the expense of relatively reduced bandwidth and range. In contrast, both Frequency Modulated (FM) modes provide fundamentally unlimited measurement bandwidth and wide linear input range at the expense of resolution. The switching between AM and FM is necessary when high dynamic range measurements are required. To implement a switching logic electronically, the required noise resolution together with the maximum input range can serve as a criteria for selection of the correct operating mode. For low noise operation, the AM mode is optimal, while for high bandwidth and wide input range, the FM is preferred. The final choice between FM and WA depends on whether angular rate or positioning angle output is required.

6. Conclusion

We demonstrated the interchangeable operation of a silicon MEMS Coriolis vibratory gyroscope capable of precision and wide range measurements of the angular rate and angle of rotation. The vacuum sealed SOI prototype with a 2 kHz operational frequency demonstrated virtually identical X- and Y-mode Q-factors of 1.2 million (with $\Delta Q/Q$ of 1%), approaching the thermoelastic limit of 1.3 million. This allows for a power failure-independent operation with polarization voltages as low as 10 mV dc previously achieved only in HRG for space-flight missions [21]. Due to stiffness and damping symmetry, and ultra-low dissipation, this gyroscope was instrumented for the precision rate and angle measurements in high bandwidth and range. The QMG gyroscope experimentally demonstrated a 0.1 °/hr bias instability in rate measuring mode, a 18,000 °/s linear input range. Temperature characterization of the transducer also revealed less than 0.2 % variation of the angular rate response between 25 °C and 70 °C environments, enabled by the self-calibration due to differential frequency detection. Interchangeable operation of the QMG transducer provides a measured 176 dB dynamic range, making the same high-Q mechanical structure suitable for demanding high precision and wide input range applications.

7. Acknowledgement

This work was supported by the Office of Naval Research and Naval Surface Warfare Center Dahlgren Division under Grants N00014-09-1-0424 and N00014-11-1-0483. The authors would like to thank the staff of the UCLA Nanoelectronics Research Facility and SST International for assistance with vacuum packaging, Dr. Flavio Heer from Zurich Instruments AG for assistance with the signal processing, and Ilya Chepurko for assistance with the frontend PCB. The gyroscopes were designed, developed, and characterized at the MicroSystems Laboratory, University of California, Irvine.

8. References

[1] A. M. Shkel, “Type I and Type II micromachined vibratory gyroscopes,” in Proc. IEEE/ION Position Location and Navigation Symposium (PLANS), San Diego, CA, Apr. 24–27, 2006, pp. 586–593.

[2] D. Lynch, “Coriolis Vibratory Gyros,” in Symposium Gyro Technology, 1998, pp. 1.0–1.14. Reproduced as Annex B, Coriolis Vibratory Gyros, pp. 56–66 of IEEE Std. 1431–2004. IEEE Standard Specification Format Guide and Test Procedure of Coriolis Vibratory Gyros, IEEE Aerospace and Electronic Systems Society, 20 December, 2004.

[3] A. Shkel, “Microtechnology comes of age,” GPS World, pp. 43–50, 2011.

[4] M. Zaman, A. Sharma, Z. Hao, and F. Ayazi, “A mode-matched silicon yaw tuning-fork gyroscope with subdegree-per-hour Allan deviation bias instability,” IEEE/ASME Journal of Microelectromechanical Systems, vol. 17, no. 6, pp. 1526 –1536, Dec. 2008.

[5] B. R. Johnson, E. Cabuz, H. B. French, and R. Supino, “Development of a MEMS gyroscope for northfinding applications,” in Proc. IEEE/ION Position Location and Navigation Symposium (PLANS), May 2010, pp. 168–170.

[6] E. Tatar, S. Alper, and T. Akin, “Effect of quadrature error on the performance of a fully-decoupled mems gyroscope,” in IEEE Proc. Micro Electro Mechanical Systems (MEMS), Jan. 2011, pp. 569 –572.

[7] I. Prikhodko, S. Zotov, A. Trusov, and A. Shkel, “Sub-degree-perhour silicon MEMS rate sensor with 1 million Q-factor,” in Proc. 16th International Conference on Solid-State Sensors, Actuators and Microsystems (TRANSDUCERS’11), Beijing, China, Jun. 5–9, 2011, pp. 2809–2812.

[8] B. Chaumet, B. Leverrier, C. Rougeot, and S. Bouyat, “A new silicon tuning fork gyroscope for aerospace applications,” in Symposium Gyro Technology 2009, Karlsruhe, Germany, Sep.22–23, 2009, pp. 1.1–1.13.

[9] W. Geiger, J. Bartholomeyczik, U. Breng, W. Gutmann, M. Hafen, E. Handrich, M. Huber, A. Jackle, U. Kempfer, H. Kopmann, J. Kunz, P. Leinfelder, R. Ohmberger, U. Probst, M. Ruf, G. Spahlinger, A. Rasch, J. Straub-Kalthoff, M. Stroda, K. Stumpf, C. Weber, M. Zimmermann, and S. Zimmermann, “MEMS IMU for ahrs applications,” in Proc. IEEE/ION Position Location and Navigation Symposium (PLANS), May 2008, pp. 225 – 231.

[10] Anthony D. Challoner, Howard H. Ge, and John Y. Liu, “Boeing Disc Resonator Gyroscope”, in Proc. IEEE/ION Position Location and Navigation Symposium (PLANS), May, 2014, pp. 504 – 514.

[11] A. Trusov, I. Prikhodko, S. Zotov, A. Schofield, and A. Shkel, “Ultrahigh Q silicon gyroscopes with interchangeable rate and whole angle modes of operation,” in IEEE Proc. Sensors, 2010, pp. 864–867.

[12] A. Trusov, I. Prikhodko, S. Zotov, and A. Shkel, “Low-dissipation silicon tuning fork gyroscopes for rate and whole angle measurements,” IEEE Sensors Journal, 2011, vol. 11, no. 11, pp. 2763–2770.

[13] S. Zotov, A. Trusov, and A. Shkel, “Experimental demonstration of a wide dynamic range angular rate sensor based on frequency modulation,” in IEEE Proc. Sensors, Limerick, Ireland, Oct. 28–31, 2011.

[14] I. Prikhodko, S. Zotov, A. Trusov, and A. Shkel, “Foucault pendulum on a chip: Angle measuring silicon MEMS gyroscope,” in IEEE Proc. Micro Electro Mechanical Systems (MEMS), Cancun, Mexico, Jan. 23–27, 2011, pp. 161–164.

[15] S. A. Zotov, A. A. Trusov, and A. M. Shkel, “High-range angular rate sensor based on mechanical frequency modulation,” IEEE/ASME Journal of Microelectromechanical Systems, no. 99, pp. 1 – 8, 2012.

[16] A. A. Trusov, A. R. Schofield, and A. M. Shkel, “Micromachined tuning fork gyroscopes with ultra-high sensitivity and shock rejection,” U.S. Patent Application 20 100 313 657.

[17] Igor P. Prikhodko, Brenton R. Simon, Gunjana Sharma, Sergei A. Zotov, Alexander A. Trusov, and Andrei M. Shkel, “High and Moderate Level Vacuum Packaging of Vibratory MEMS,” 46-th International Symposium on Microelectronics (IMAPS), Orlando, FL, USA, September 30 – October 3, 2013, pp. 705 – 710.

[18] B. Kim, M. Hopcroft, R. Candler, C. Jha, M. Agarwal, R. Melamud, S. Chandorkar, G. Yama, and T. Kenny, “Temperature dependence of quality factor in MEMS resonators,” IEEE/ASME Journal of Microelectromechanical Systems, vol. 17, no. 3, Jun. 2008. pp. 755–766.

[19] Sergei A. Zotov, Brent R. Simon, Igor P. Prikhodko, Alexander A. Trusov, Andrei M. Shkel, “Quality Factor Maximization through Dynamic Balancing of Tuning Fork Resonator” IEEE Sensors Journal, vol. 14, no. 8, , Aug. 2014, pp. 2706 – 2714.

[20] M.A. Hopcroft, W.D. Nix, T.W. Kenny, “What is the Young’s modulus of silicon?,” IEEE/ASME Journal of Microelectromechanical Systems, vol. 19, no 2, 2010 Apr, pp. 229–238.

[21] D. M. Rozelle, “The hemispherical resonator gyro: From wineglass to the planets (AAS 09-176),” in Proc. 19th AAS/AIAA Space Flight Mechanics Meeting, Feb. 2009, pp. 1157–1178.